Radiotherapy and Oncology 206 (2025) 110784

Contents lists available at ScienceDirect

Radiotherapy and Oncology

journal homepage: www.thegreenjournal.com

Original Article

Consensus for a postoperative atlas of sinonasal substructures from a modified Delphi study to guide radiotherapy in sinonasal malignancies

Florent Carsuzaa [a,b,*], Valentin Favier [c,d,*], Lise Seguin [a], Mario Turri-Zanoni [e], Anna-Maria Camarda [f,g], Benjamin Verillaud [h], Philippe Herman [h], Daniele Borsetto [i], Alberto Schreiber [j], Stefano Taboni [k], Vittorio Rampinelli [j], Alessandro Vinciguerra [h], Alperen Vural [l], Xavier Liem [m], Fabio Busato [n], Sophie Renard [o], Charles Dupin [p,q], Mélanie Doré [r], Pierre Graff [s], Yungan Tao [t], Séverine Racadot [u], Antoine Moya Plana [v], Basile N. Landis [w], Pierre-Yves Marcy [x], Vincent Patron [y], Ludovic de Gabory [z], Ester Orlandi [f,1], Marco Ferrari [k,1], Juliette Thariat [aa,ab,1]

[a] Department of Otolaryngology – Head & Neck Surgery, University Hospital of Poitiers, Poitiers, France
[b] LITEC UR15560, University of Poitiers, Poitiers, France
[c] Department of Otolaryngology – Head & Neck Surgery, Hospital Gui de Chauliac, University Hospital of Montpellier, Montpellier, France
[d] Research-team ICAR, Laboratory of Computer Science, Robotics and Microelectronics of Montpellier (LIRMM), University of Montpellier, French National Centre for Scientific Research (CNRS), Montpellier, France
[e] Division of Otorhinolaryngology, Department of Biotechnology and Life Sciences, University of Insubria, ASST Lariana, Como, Italy
[f] Clinical Department, National Center for Oncological Hadrontherapy (Fondazione CNAO), Pavia, Italy
[g] Department of Clinical, Surgical, Diagnostic, and Pediatric Sciences, University of Pavia, Pavia, Italy
[h] Otorhinolaryngology and Skull Base Center, AP-HP, Hospital Lariboisière, Paris, France
[i] Department of ENT, Cambridge University Hospitals NHS Trust, United Kingdom
[j] Unit of Otorhinolaryngology Head and Neck Surgery, ASST Spedali Civili Brescia, Department of Medical and Surgical Specialties, Radiological Sciences, and Public Health, University of Brescia, Brescia, Italy
[k] Section of Otorhinolaryngology Head and Neck Surgery, Department of Neurosciences, University of Padua, Padua, Italy
[l] Department of Otolaryngology – Head & Neck Surgery, Istanbul University Cerrahpasa – Cerrahpasa Faculty of Medicine, Istanbul, Turkey
[m] Department of Radiation Oncology, Oscar Lambret Center, Lille, France
[n] Department of Radiation Oncology, Abano Terme Hospital, Padua, Italy
[o] Department of Radiation Oncology, Institut de cancérologie de Lorraine, Vandœuvre-lès-Nancy, France
[p] Department of Radiation Oncology, Bordeaux University Hospital, Bordeaux, France
[q] Bordeaux University, BRIC (BoRdeaux Institute of OnCology), UMR1312, INSERM, University of Bordeaux, Bordeaux, France
[r] Department of Radiation Oncology, Institute de cancérologie de l'Ouest (ICO) centre René-Gauducheau, Saint-Herblain, France
[s] Department of Radiation Oncology, Institut Curie, PSL Research University, Paris – Saint Cloud-Orsay, France
[t] Department of Radiation Oncology, Gustave Roussy, Villejuif, France
[u] Department of Radiation Oncology, Centre Léon Bérard, Lyon, France
[v] Department of Otolaryngology – Head & Neck Surgery, Gustave Roussy, Villejuif, France
[w] Rhinology-Olfactory Unit, Department of Otorhinolaryngology-Head and Neck Surgery, University Hospital of Geneva Medical School, Geneva, Switzerland
[x] PolyClinics ELSAN Group, Medipole Sud, Quartier Quiez, 83189 Ollioules, France
[y] Department of Otolaryngology – Head & Neck Surgery, University Hospital of Caen, Caen, France
[z] Department of Otolaryngology and Head & Neck Surgery, Bordeaux University Hospital, Bordeaux, France
[aa] Centre François Baclesse, Comprehensive Cancer Center, Caen, France
[ab] Laboratoire de physique Corpusculaire IN2P3/ENSICAEN/CNRS UMR 6534, Normandie Université, Caen France

ARTICLE INFO

Keywords:
Skull base
Sinonasal malignancies

ABSTRACT

Background: Sinonasal and skull base tumor surgery-related morbidity has been reduced by the use of endoscopic endonasal skull base surgery (EESBS). Postoperative radiation therapy (poRT) requires precise definition of

* Corresponding authors at: Department of Otorhinolaryngology, University Hospital of Poitiers, 2 rue de la Milétrie, F-86000 Poitiers, France (F. Carsuzaa). Otolaryngology, Head and Neck surgery Departement, University Hospital of Montpellier, 80 Avenue Augustin Fliche, 34000 Montpellier, France (V. Favier).
E-mail addresses: florent.carsuzaa@gmail.com (F. Carsuzaa), valentin_favier@hotmail.com (V. Favier).
[1] Equally contributed to the study as co-last authors.

https://doi.org/10.1016/j.radonc.2025.110784
Received 20 August 2024; Received in revised form 30 January 2025; Accepted 10 February 2025
Available online 20 February 2025

Radiotherapy
Dose-painting

target volumes. To enhance the accuracy of poRT planning, histological and radiological correlations are necessary to locate the tumor attachment on poRT CT scans. An accurate atlas of structures resected or identified during EESBS could serve for the interdisciplinary postoperative management of patients, personalizing poRT by adequate radiation dose delivery. The objective of this study was to achieve a consensual segmentation atlas on CT scan with surgeons practicing EESBS and radiation oncologists.

Methods: The sinonasal structures relevant for poRT of sinonasal malignancies were determined by a two-round Delphi process. A rating group of 25 European experts in sinonasal malignancies was set up. Consensual structures emerged and were used to determine the anatomical limits of the retained structures to draft an atlas with expert based relevant structures. The atlas was then critically reviewed, discussed, and edited by another 2 skull base surgeons and 2 radiation oncologists.

Results: After the two rating rounds, 46 structures obtained a strong agreement, 7 an agreement, 5 were rejected and 5 did not reach consensus. The atlas integrating all the selected structures is presented attached.

Conclusion: Consensual segmentation atlas on CT scan might allow, through careful poRT planning to limit the morbidity of poRT while maintaining good local control. Prospective studies are necessary to validate this potential precision medicine-based approach.

Introduction

Sinonasal and skull base tumor surgery-related morbidity in sinonasal malignancies has been reduced in the past decades with the evolution of endoscopic endonasal skull base surgical (EESBS) procedures, with equivalent oncological outcomes to open approaches [1–6]. Postoperative radiation therapy (poRT), often necessary as an adjuvant modality with or without concomitant chemotherapy, has dramatically evolved in the last two decades with the implementation of simultaneous integrated boost RT through intensity-modulated RT (IMRT), volumetric modulated arc therapy (VMAT), and proton RT (PT) [7,8]. Although sharp dose profiles usually achieved with these techniques, with special reference to PT, allow for better tumor dose conformity, they are also more susceptible to topographical misses. This susceptibility is amplified when considering the elevated anatomical uncertainties, especially with PT. Thus, the precise definition and delineation of target tumor volumes are crucial in modern RT.

EESBS operative report can be used to provide a detailed and accurate mapping of the sinonasal and skull base tumor involvement. The precise identification of tumor location is also a key factor to understand the anatomical tumor involvement, and the quality of surgical resection margins, especially in the era of EESBS due to no monobloc resection. Orbital preservation best represents the compromise made to achieve acceptable oncological results while maximizing functional outcomes [9].

Sinonasal tumors are often pedicled, with a large intraluminal compartment bulging into the cavities and pushing or destroying surrounding structures. EESBS allows to visualize the pedicle tumor site and its extension, which can be precisely reported on standardized anatomic 3D drawings and as detailed reports [10]. Such surgeon's feedback / reports after EESBS are necessary for radiation oncologists to better locate the tumor implantation. Preoperative imaging alone may overestimate tumor involvement due to compression or inflammation caused by the bulging part of the tumor [11]. Moreover, the professionals of a multidisciplinary tumor board meeting have a different vision of anatomical structures which depends on the practical interests or constraints linked to the prism of their discipline. EESBS operative reports can also be used to accurately identify tumor involvement of anatomical structures. Finally, a better interdisciplinary communication [12] may help to personalize poRT in sinonasal malignancies by facilitating dose-painting radiotherapy, in a customized and interdisciplinary approach.

We hypothesized that standardization of operative and pathological reports could assist radiation oncologists in achieving this goal, by improving the delineation of tumor margins and dissemination pathways on postoperative CT scans. To further enhance the precision of poRT planning, accurate histo-radiological correlation is relevant to locate each fragment on successive planar images from the radiotherapy planning scanner. The determination of volumes to be irradiated is typically based on pre-operative imaging, operative and pathological reports, and knowledge of anatomical extensions [13]. An accurate radio-anatomical segmentation atlas (i.e., anatomical region of interest delineated on a CT scan) of structures resected or identified during EESBS could serve for the interdisciplinary postoperative management of patients with sinonasal tumors, but none exists in the current literature.

The objective of this study was to achieve a consensual segmentation atlas on CT scan, using a modified Delphi method applied to a committee of EESBS surgeons and radiation oncologists.

Methods

Definition of sinonasal structures

The sinonasal structures relevant for poRT in sinonasal malignancies were determined by a two-round Delphi process [14]. The Delphi methodology is an iterative process used to achieve consensus from different opinions on open questions that are not sufficiently supported by evidence (Fig. 1). A steering committee (SC) of 5 experts (2 radiation oncologists: JT, EO; and 3 EESBS surgeons: FC, VF, MF) was tasked with identifying relevant sinonasal structures. The initial list of structures was established from an anatomical diagram for sinonasal malignant tumor resection reporting published by Bastier et al. (n = 24) [10], to which relevant contiguous structures were added.

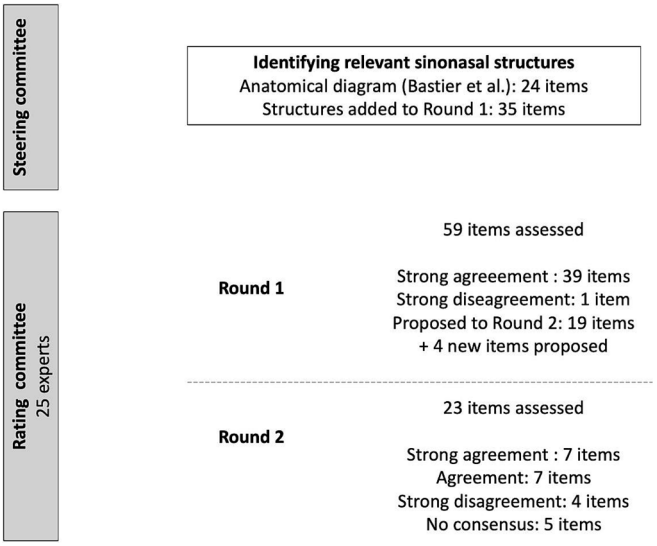

Fig. 1. Overview of the two rounds Delphi process.

Definition of consensus and outliers' management

In the first round, the experts had to rate the statements between 1 and 9 (1: totally disagree; 9: totally agree), as recommended in the guidelines of the French Health Authority [15] (Table 1). For a cohort comprising over 16 experts, the initial round of analysis allows for the omission of either two missing values or two values that diverge from the majority of the group. Strong positive and negative agreements emerged. For other items without consensus, the SC provided an anonymized summary of the experts' opinions from the first round as well as the reasons they provided their judgments. The panel had to revise their early replies considering the replies of the other experts. After this second round, strong agreements and agreements emerged (Table 1). Similarly to the first round, the analysis in the second round allows for the omission of two missing values or two values that are contrary to the majority of the group.

Creation of the sinonasal subunit atlas

After having determined the anatomical limits of the retained structures, a draft atlas was first generated by 2 skull base surgeons (FC, LS), 1 radiation oncologist (JT), and 1 neuroradiologist (PYM). Delineation of sinonasal structures was performed on CT scans from healthy patients (whose CT scans were considered normal, acquired with a slice thickness of 1 mm or less) with the help of 3D MR sequences (acquired with a 2 mm slice thickness or isotropic voxel size) using RayStation® V12 (RaySearch Laboratories, Stockholm, Sweden). The atlas was then critically reviewed, discussed, and edited by another 2 skull base surgeons (VF, MF) and 2 radiation oncologists (EO, AMC). The final atlas resulted from a consensus of all the investigators.

Statistics

Quantitative variables are presented as medians with interquartile ranges (IQR). Comparisons between the responses of surgeons and radiation oncologists were compared using Student *t*-test. All statistical analyses were performed using R (version 3.3.2).

Table 1
Proposals accepted after the first and second round depending on median value and distribution of quotes.

First round				
Proposal judged		**Median value**	**Distribution of quotes**	**Subjected to the second round**
Appropriate	Strong consensus	≥7	All the quotes between [7–9]	No, recommendation accepted
	Consensus	≥7	All the quotes between [5–9]	Yes
Inappropriate	Strong consensus	≤3	All the quotes between [1–3]	No, recommendation rejected
	Consensus	≤3.5	All the quotes between [1–5]	Yes
Uncertain	Lack of consensus	All the other situation		No

Second round			
Proposal judged		**Median value**	**Distribution of quotes**
Appropriate	Strong consensus	≥7	All the quotes between [7–9] except 2 missing or < 7
	Consensus	≥7	All the quotes between [5–9] except 2 missing or < 7
Inappropriate	Strong consensus	≤3	All the quotes between [1–3] except 2 missing or > 3
	Consensus	≤3.5	All the quotes between [1–5] except 2 missing or > 5

Results

A group of 25 international experts in sinonasal malignancies was assembled, consisting of 15 otolaryngology and skull base surgeons and 10 radiation oncologists. They all complete the two rounds of the Delphi study.

Fifty-nine items were proposed to the rating group during the first round. At the end of the first round, 39 were accepted with strong agreement, 1 was rejected with strong agreement and 19 were proposed in the second round. During the second round, 4 new items were proposed by the panelists and were accepted with strong agreement. At the end of the two rating rounds, 46 items obtained a strong agreement, 7 an agreement, 4 were rejected and 5 did not reach consensus. The result of the two rating rounds and the details of the structures retained in the atlas are described in Table 3.

Some differences in rating between surgeons and radiation oncologists emerged. Surgeons considered the medial orbital gyrus more important than radiation oncologists (median: 6 vs 3.4; $p = 0.0074$). Surgeons tended to consider the vertebrae C1-C2 ($p = 0.78$), Eustachian tube ($p = 0.78$), optic canal ($p = 0.27$), pterygoid canal, lower ($p = 0.07$) and middle ($p = 0.06$) clivus, gyrus rectus ($p = 0.57$), crista galli ($p = 0.26$), olfactory cleft ($p = 0.18$), cribriform plate ($p = 0.07$), and frontal process of maxilla ($p = 0.77$) more important to include in the atlas than radiation oncologists. Radiation oncologists tended to consider superior turbinate and nasopharyngeal walls more important than surgeons ($p = 0.07$ and $p = 0.32$, respectively). The limits of the anatomical structures retained are defined in Table 2.

The atlas integrating all the selected structures has been built and is presented in overall view in Figs. 2 and 3 and in its entirety in **Supplementary Material** [16].

Discussion

The comparatively lower morbidity rate associated with EESBS, relative to traditional open approaches, can be effectively combined with modern radiation modalities to offer individual therapeutic options with reduced complications while maintaining high efficacy [17,18]. In poRT planning for sinonasal malignancies, the virtual transfer of sinonasal tumor location from preoperative views to postoperative axial CT is crucial during the delineation phase. This process is pivotal not only to the accurate delineation of the macroscopic disease but also for selecting target volumes at risk of harboring microscopic disease, informed by histopathological data.

EESBS represents a significant shift for radiation oncologists, necessitating thorough documentation and understanding of tumor extents and quality of surgical margins to ensure effective tumor control. EESBS resection results in the piecemeal resection into smaller tissue fragments, often measuring only a few millimeters. Surgeons typically annotate and orient each of these fragments [10]. It is key to standardize the orientation of surgical sampling and the resection of anatomical areas. Operative reports, whether graphical or textual, serve as the foundation for a universal language among all specialties involved in managing patients with sinonasal tumors. These reports enable pathologists to identify safe tissue fragments, tumor sub-volumes, and assess the quality of tumor margins and additional surgical margins. Their analysis is crucial for evaluating margin quality and informing the radiation oncologists about the prescribed dose [19]. Post-operative imaging relies on radiotherapy CT. Additional imaging, such as MRI, is not standard practice; it might become more systematic in the future to address postoperative changes and it may be recommended in case of gross disease. The use of segmentation atlases of the sinonasal subunits would make it possible to better harmonize the reporting of areas resected during surgery and those at risk and make it possible to consider dose-painting poRT adapted to patients and their tumors' characteristics. The consensus guidelines developed by Grégoire et al. and Brouwer et al. underscore the importance of standardizing target

Table 2
Anatomic definition of retained structures.

Segmentation	Pair or single	Radiological definition
Nasal bone	Pair	Bone located the more anteriorly in the face, in connection with the frontal, ethmoid perpendicular plate, and maxilla bones
Nasal septum	Single	Composed of perpendicular plate of septal cartilage, ethmoid perpendicular plate, premaxilla-maxillary crest and vomer bone.
Nasal floor	Pair	Lower boundary of the nasal fossa, which constitute the medial part of the hard palate. It is composed by the horizontal process of the maxillary bone anteriorly and the horizontal process of the palatine bone posteriorly. Anterior limit: anterior nasal spine; Posterior limit: posterior border of the palatine bone horizontal process
Inferior turbinate	Pair	Composed of a separate bone covered by mucosa that articulates with the inferior margin of the maxillary hiatus. It is also connected with the uncinate process upward, the vertical process of the maxillary bone anteriorly the vertical lamella of the palatine bone posteriorly.
Middle turbinate	Pair	Composed by the head, the body and the tail of the middle turbinate. Medially and superiorly has a vertical attachment to the skull base at the lateral border of the cribriform plate. The vertical attachment is in a paramedian sagittal plane. At mid road, this attachment rotates 90° to follow transversely the ethmoid roof and to reach the lamina papyracea close to the orbit. This is the basal lamella of the middle turbinate which separates the ethmoid labyrinth in anterior and posterior group relative to the basal lamella.
Medial maxillary wall	Pair	Bone component of the medial maxillary sinus wall
Anterior maxillary wall	Pair	Bone component of the anterior maxillary sinus wall excluding the sinus floor and roof
Posterolateral maxillary wall and sinus floor	Pair	Bone component of the posterior, lateral, and inferior wall of the sinus (with dental roots)
Medial orbital wall	Pair	Bone component of the medial wall of the orbit. Composed by the lacrymal bone anteriorly and the lamina papyracea posteriorly: smooth, oblong bone plate which forms the lateral surface of the labyrinth of the ethmoid bone. The frontal bone allows the junction between the medial orbital wall and the roof.
Orbital roof	Pair	Bone component of the superior wall of the orbit. In case of lateral pneumatization of the frontal sinus, the orbital roof form the floor of the frontal sinus anteriorly. Posteriorly, the orbital roof is the lateral part of the anterior cranial fossa
Orbital floor	Pair	The inferior wall of the orbit. Formed by the orbital surface of the maxilla, the orbital surface of the zygomatic bone, the orbital process of the palatine bone. The floor is separated from the posterior wall by the inferior orbital fissure, which connects the orbit to pterygopalatine and infra-temporal fossa.
Medial rectus muscle	Pair	Oculomotor muscle located laterally to the medial orbital wall
Frontal process of the maxilla	Pair	Part of the maxillary bone forming the anterior part of the nasal fossa and frontal sinus. It articulates with nasal bones anteriorly, with the ethmoid and frontal bones anteriorly, with the lacrymal bone posteriorly
Lacrimal sac and nasolacrimal duct	Pair	The lacrimal sac receives the common canaliculus of the lacrimal drainage system, formed from the union of the superior and inferior canaliculi. The sac lies within the lacrimal fossa of the medial orbital wall. The nasolacrimal duct leaves the inferior aspect of the lacrimal sac, runs inferiorly and enters the inferior meatus approximately 10–15 mm from the head of the inferior turbinate. The nasolacrimal tract includes the bone (unguis and vertical process of the maxillary bone)
Internal canthus	Pair	Skin in front of the lacrimal sac
Infraorbital foramen	Pair	Foramen located in the anterior wall of maxillary sinus, forming the anterior end of the infraorbital canal which transmits the infraorbital nerve and vessels.
Anterior ethmoid	Pair	Cells located anteriorly to the basal lamella to the vertical process of the maxillary bone
Posterior ethmoid	Pair	Cells located posteriorly to the basal lamella and anteriorly to the anterior wall of the sphenoid (not including the bony part of the sphenoid)
Ethmoid roof	Pair	In coronal view, between the orbital plate of the frontal bone, and the vertical lateral lamella laterally and the cribriform plate medially
Cribriform plate	Pair	Bordered anteriorly by the inferior aspect of the frontal bones, posteriorly by the sphenoid planum, medially by the nasal septum and laterally by the superior and middle turbinates.
Olfactory cleft	Pair	Air space located between the middle and superior turbinate laterally, the nasal septum medially, the cribriform plate and the sphenoid planum superiorly, the anterior wall of the sphenoid sinus posteriorly. The inferior border of this space is virtual and projects at the level of the lower edge of the middle turbinate
Olfactory fossa	Pair	Medial part of the anterior cranial fossa located above the cribriform plate, where the olfactory bulb take place. The two olfactory fossae are separated by the crista galli anteriorly.
Superior turbinate	Pair	Composed by the head, the body and the tail of the superior turbinate. Superiorly has a vertical attachment to the skull base at the lateral border of the cribriform plate, posterior to the middle turbinate insertion. The vertical attachment is in a paramedian sagittal plane. The basal lamella is an attachment to the nasal lateral wall.
Frontal sinus anterior wall	Pair	Bone component of the anterior frontal sinus wall.
Frontal sinus posterior wall	Pair	Bone component of the frontal sinus posterior wall, which constitute the anterior wall of the anterior cranial fossa.
Crista galli	Single	Intracranial component of the ethmoid bone, located behind the foramen caecum, between the both cribriform plates and extending superiorly close to the sagittal veinous sinus. Its anterior border is posterior to the frontal sinus posterior wall.
Sphenoid intersinus septum	Single	Bone component of the sphenoid sinus medial walls, separating the sphenoid in two sphenoid sinuses.

(*continued on next page*)

Table 2 (*continued*)

Segmentation	Pair or single	Radiological definition
Sphenoid sinus anterior wall	Pair	Bone component of the sphenoid sinus anterior wall, between the nasal septum and the medial wall of the orbit. Its medial single extension is the *rostrum sphenoidale*, which articulates with the vertical plate of the vomer
Sphenoid sinus lateral wall	Pair	Bone component of the sphenoid sinus lateral wall
Sphenoid sinus superior wall	Pair	Bone component of the sphenoid sinus superior wall (planum sphenoidale)
Middle clivus	Single	Bone component of the clivus located at the posterosuperior border of the nasopharynx, below the sella turcica, from the glossopharyngeal nerve to the foramen magnum
Inferior clivus	Single	Inferior part of the clivus located posteriorly to the nasopharynx between the exits of the trigeminal and the glossopharyngeal nerves
Cavernous sinus	Pair	Venous structure located in close contact with the lateral wall of the sphenoid sinus, allowing the pathway for oculomotor nerves and internal carotid artery. Cavernous sinuses are on either side of the sella turcica and pituitary gland
Meckel's cave	Pair	Posterolateral to the cavernous sinus on either side of the sphenoid bone. Medial to the ganglion in Meckel's cave is the internal carotid artery in the posterior portion of the cavernous sinus. Inferior is the motor root of the trigeminal nerve and the petrous apex of the petrous temporal bone with the internal carotid artery traversing the carotid canal.
Foramen rotundum	Pair	Located in the middle cranial fossa, inferomedial to the superior orbital fissure at the base of greater wing of the sphenoid bone. Its medial border is formed by lateral wall of sphenoid sinus. It runs downwards and laterally in an oblique path and joins the middle cranial fossa with the pterygopalatine fossa.
Foramen ovale	Pair	An oval shaped opening in the middle cranial fossa located at the posterior base of the greater wings of the sphenoid bone, lateral to the lingula, posterolateral to the foramen rotundum.
Carotid canal	Pair	Passage within the petrous temporal bone that transmits the internal carotid artery. Its inferior opening is called the carotid foramen and is situated anteriorly to the jugular fossa and medially to the carotid plate. The carotid canal is initially directed superiorly, then turns anteromedially to reach up to the petrous apex. It runs approximately 2 cm within the petrous bone and opens into the middle cranial fossa superior to the foramen lacerum.
Pterygoid (Vidian) canal	Pair	Located in the pterygoid process of the sphenoid bone, superior to the pterygoid plates, and inferomedial to the foramen rotundum. Its position relative to the sphenoid sinus is dependent on the pneumatisation of the sinus so that the nerve may be encased in the basisphenoid bone, partially protruding into the sinus floor or occasionally exposed within the sinus cavity and connected to the floor by a bony stalk.
Superior orbital fissure	Pair	This fissure is of a triangular shape, and leads from the cavity of the cranium into that of the orbit. It is bounded: • medially by the body of sphenoid; • above, by the lesser wing of sphenoid; • below, by the medial margin of the orbital surface of the great wing; • and is completed laterally by the frontal bone
Inferior orbital fissure	Pair	In the floor of the orbit, inferior to the superior orbital fissure and bounded superiorly by the greater wing of sphenoid, inferiorly by the maxilla and the orbital process of palatine bone and laterally by the zygomatic bone. It opens into the posterolateral aspect of orbital floor.
Optic canal	Pair	Cylindrical canal running obliquely through the area where the lesser wing of sphenoid bone joins the body of sphenoid.
Infratemporal fossa (or deep masticator space)	Pair	Between the ramus of the mandible laterally and the superior constrictor muscles of the pharynx and the lateral pterygoid plate medially
Pterygopalatine fossa	Pair	Its anterior boundary is the posterior wall of the maxilla, and posteriorly is the base of the pterygoid process and the greater wing of the sphenoid bone. Its roof is the body of the sphenoid bone with the orbital process of the palatine bone, and the floor comprises the pyramidal process of the palatine bone with the lateral pterygoid plate
Lesser wings of the sphenoid	Pair	Part of the sphenoid bone located between the planum sphenoidale and the greater wing of the sphenoid. It is the superior boundary of the superior orbital fissure. It can be partially pneumatized.
Greater wing of the sphenoid	Pair	Sphenoid bone lateral to sphenoid body and superior to pterygoid process. It can be partially pneumatized.
Pterygoid plates	Pair	Bone component of the pterygoid process separated in medial and lateral plates. The medial plate of the pterygoid forms the lateral part of the choana
Base of the pterygoid process	Pair	Upper part of the pterygoid process at the junction of the sphenoid bone body and greater wing. Ends with the separation of pterygoid plates. It surrounds the pterygoid canal and foramen rotundum.
Posterior wall of the nasopharynx	Single	Mucosal, muscular, and fascial component of the posterior wall of the nasopharynx, located anteriorly to the clivus and C1-C2
Lateral wall of the nasopharynx	Pair	Mucosal, muscular, fascial, and cartilaginous component the lateral wall of the nasopharynx. It comprises the cartilaginous Eustachian tube
Roof of the nasopharynx	Single	Mucosal component of the superior wall of the nasopharynx, located inferiorly to the sphenoid body
Gyrus rectus (brain)	Pair	Most medial and inferior part of the frontal lobe. It is bounded medially by the interhemispheric fissure, and is separated laterally by the inferior rostral sulcus

volume delineation in head and neck oncology to minimize treatment variability and improve clinical outcomes [20,21]. However, they didn't include the sinonasal region in the atlas description, leading to a remaining gap to standardize PORT delineation in this area. Their work provides a foundation for systematic radiotherapy planning, emphasizing anatomical precision, particularly in regions of complex anatomical variability such as the sinonasal and skull base areas. This aligns closely with the objectives of our atlas, which seeks to bridge surgical observations and radiotherapeutic needs. Furthermore, the integration of histopathological insights into radiotherapy planning, as

Table 3
Results of the two rounds of Delphi process.

Structure	1st round Med [IQ]	2nd round Med [IQ]	Structure	1st round Med [IQ]	2nd round Med [IQ]
Nasal bone	9 [3–9]		Anterior sphenoidal wall*	9 [6–9]	
Nasal septum*	9 [2–9]		Lateral sphenoidal wall	9 [7–9]	
Nasal floor*	9 [7–9]		Posterior sphenoidal wall	9 [8,9]	
Inferior turbinate*	8 [3–9]		Middle clivus	8 [3–9]	
Middle turbinate*	7 [1–9]	8 [2–9]	Inferior clivus	8 [3–9]	
Medial maxillary wall*	8 [5–9]		Superior clivus	8 [3–9]	3 [1–8]
Anterior maxillary wall*	9 [7–9]		Cavernous sinus		9 [5–9]
Posterolateral maxillary wall*	9 [7–9]		Meckel's cave		9 [3–9]
Uncinate process*	5 [1–9]	3 [1–8]	Foramen rotundum	9 [7–9]	
Medial orbital wall	9 [8,9]		Foramen ovale	9 [7–9]	
Orbital roof	9 [3–9]		Carotid canal	9 [5–9]	
Orbital floor*	9 [5–9]		Pterygoid canal (vidian canal)	9 [3–9]	
Medial rectus muscle	8 [3–9]	8 [2–9]	Superior orbital fissure	9 [3–9]	
Frontal process of maxilla	7 [3–9]	7 [2–9]	Inferior orbital fissure	9 [7–9]	
Nasolacrimal sac and duct*	8 [3–9]		Optic canal	9 [1–9]	
Internal canthus		8 [2–9]	Infratemporal fossa	9 [8,9]	
Inferior rectus muscle*	6 [2–9]	3 [1–8]	Temporal fossa		9 [5–9]
Infraorbital foramen*	9 [5–9]		Pterygopalatine fossa	9 [7–9]	
Anterior ethmoid*	9 [5–9]		Greater wing of sphenoid	8 [3–9]	6 [1–9]
Posterior ethmoid*	9 [5–9]		Lesser wings of sphenoid	8 [3–9]	8 [3–9]
Ethmoidal roof*	9 [7–9]		Pterygoid plates	9 [4–9]	8 [3–9]
Cribriform plate*	9 [8,9]		Base of the pterygoid process	8 [2–9]	8 [2–9]
Olfactory cleft*	9 [5–9]		Vertebrae C1-C2	7 [1–9]	5 [2–9]
Olfactory fossa*	8 [1–9]	8 [3–9]	Posterior wall of the rhinopharynx	8 [3–9]	
Superior turbinate*	7 [4–9]	7 [2–9]	Lateral wall of the rhinopharynx	8 [3–9]	
Frontal recess*	8 [2–9]	6 [2–9]	Rosenmuller fossa	3 [1–8]	
Anterior wall frontal sinus	9 [7–9]		Roof of the rhinopharynx	8 [3–9]	
Posterior wall frontal sinus	9 [7–9]		Medial ostium of the Eustachian tube*	7 [1–9]	4 [1–9]
Inferior wall frontal sinus*	9 [7–9]		Eustachian tube	8 [1–9]	5 [2–8]
Crista galli*	8 [3–9]	8 [3–9]	Gyrus rectus (brain)	8 [3–9]	8 [2–9]
Sphenoid intersinus septum	9 [7–9]		Medial orbital gyrus (brain)	8 [1–9]	6 [1–9]
Superior sphenoidal wall	9 [7–9]				

strong agreement; agreement; no consensus; strong disagreement.
*: structures proposed by Bastier et al.

outlined by these guidelines, supports the validation of our approach to creating a more personalized and effective postoperative treatment framework [20,21].

The presented consensus study identified 53 structures for which experts recommended delineation from the framework of sinonasal and skull base malignancies. These structures were identified according to endoscopic landmarks, easily identifiable anatomical regions on imaging, known tumor extension pattern and their relevance for poRT purpose. There were some differences between surgeons and radiation oncologists. Surgeons favored anatomical structures considered as essential landmarks for the surgical excision of skull base tumors. These landmarks included the C1 and C2 vertebrae and the lower and middle clivus which are often the limits of posterior excision of the tumors. However, the C1-C2 vertebrae were not consensual after adding the opinions of radiation oncologists. Probably, this is linked to the fact that these structures are easily recognizable in images from poRT CT simulation. The Eustachian tube was considered more relevant among surgeons because it represents the lateral limit of excision when the nasopharyngeal walls are involved, as well as a potential dissemination way towards the lateral skull base [22]. Another reason may be that Eustachian tube resection or irradiation is often the source of otitis media with effusion [23]. The relevance of the anatomical structure of the nasopharynx for the radiation oncologist may be linked to a greater familiarity with this structure, as it is the site of the primary tumor of the nasopharynx. Additionally, the anatomical complexity [24,25] associated with the presence of nerves, whose irradiation can lead to severe late toxicity, further emphasizes its significance [26–28]. The intracranial structures (medial orbital gyrus, gyrus rectus, crista galli), which are easily identifiable structures that can be removed according to tumor extension, were more frequently retained by surgeons. The opinions of radiation oncologists led to a lack of final consensus concerning the medial orbital gyrus. The reason for this finding may be attributed to the radiation oncologist's infrequent involvement with this structure. Specifically, since the medial orbital gyrus is separated from the gyrus rectus by the olfactory sulcus, this anatomical part may be involved mainly for olfactory neuroblastoma and adenocarcinoma. The frontal process of maxilla was also more relevant in surgeons' opinion because it can easily be individualized and because its involvement often requires a skin sacrifice [29]. The superior turbinate was more frequently retained by radiation oncologists, and it is easily individualized on imaging. This structure did not achieve a strong consensus because it requires to be grouped with the posterior ethmoid given their dissemination pathways [30]. The atlas was designed for nasoethmoid-centered tumors, which are the most common location and are less suitable for tumors of the infratemporal fossa or chordomas. We also believe that the proposed atlas may serve as a guide for a systematic analysis and standardization of sinonasal tumors extension patterns description. This atlas could then be used for imaging, surgical and pathology reports and offers a framework for detailed communication between the multidisciplinary team with the aim to allow for more precise deliver of radiation to areas of intraoperative concern or sites of historical risk for recurrence based on tumor pathology.

However, the literature lacks prospective studies concerning the reduction in morbidity made possible by better dose painting of sinonasal tumors and therapeutic de-escalation. Ongoing trials in sinonasal tumors using modern radiotherapy modalities include the French GORTEC 2016–02 phase III SANTAL trial, and the randomized phase II "SinocaRT" trial which explores de-escalation strategies in high-dose volumes, including IMRT and PT. Results from two Italian phase II trials on poor-prognosis sinonasal cancers, encompassing diverse epithelial histological subtypes, and incorporating proton and carbon ion therapy within a multidisciplinary approach, have recently been reported. While in-depth data analysis on toxicity is ongoing, the observed survival rates were similar to those reported in other series, underscoring the necessity for additional research efforts in this rare disease [26,27].

The complexity of dose distribution in poRT for sinonasal

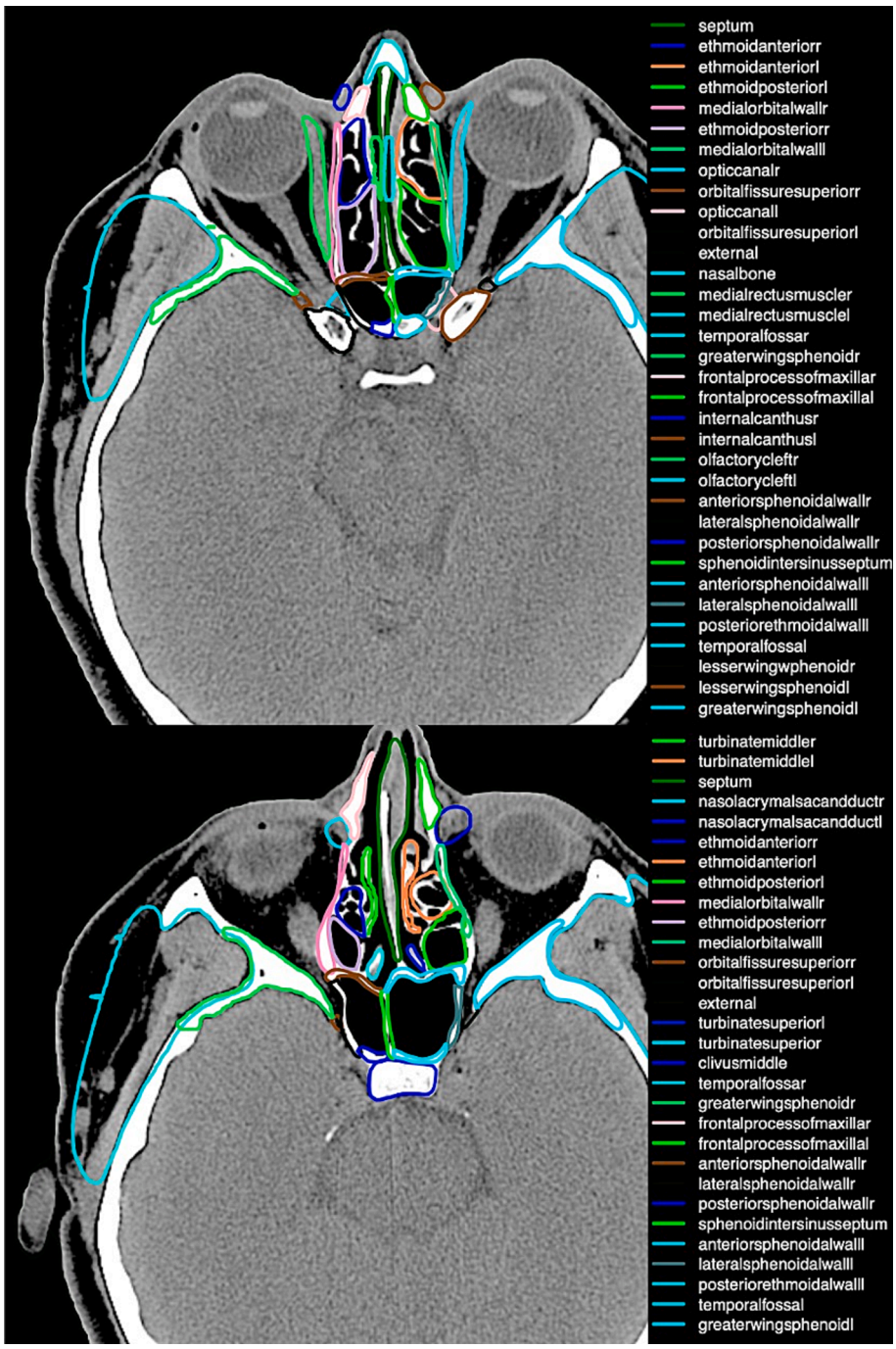

Fig. 2. Captions of the atlas centered on the ethmoid.

malignancies, with small and geometrically complex resected tumor in endoscopic techniques and surrounding structures, requires rigorous quality assurance processes [31]. In a first step, this segmentation atlas will be made automatic (ongoing process) [32]; given the number of structures, the manual delineation task would not be feasible in the busy routine clinic. Van Dijk et al. highlight the significant advancements in automatic delineation of head and neck organs at risk through deep learning contouring techniques. Their findings demonstrate that deep learning not only improves the accuracy of delineations but also reduces interobserver variability, a critical factor in complex anatomical regions like the sinonasal and skull base areas. By combining deep learning contouring with the standardized anatomical definitions of our atlas, future implementations could further refine dose-painting strategies and reduce the burden on clinicians during the delineation process [33]. However, to date, it remains difficult to train deep learning algorithms on sinonasal CT scans, as automatic segmentation and deep learning are less robust in the case of small structures. Other automatic segmentation method using less resources may be interesting to study, particularly using deformable medical image registration methods[34]. This automatic atlas will need to be adapted to the modified patient anatomy (tumor, surgery). Such adaptation is most relevantly done in tight partnership between the surgeon and the radiation oncologist. In a second step, it will serve to address the patterns of relapse more accurately than ever done. Finally, it will be necessary to group close anatomic proximity structures for which dose modulation will not be feasible in routine practice (for example, preserving the optic canal if the inferior orbital fissure is invaded by the tumor). Following such documentation, this atlas could serve to refine and likely deescalate/

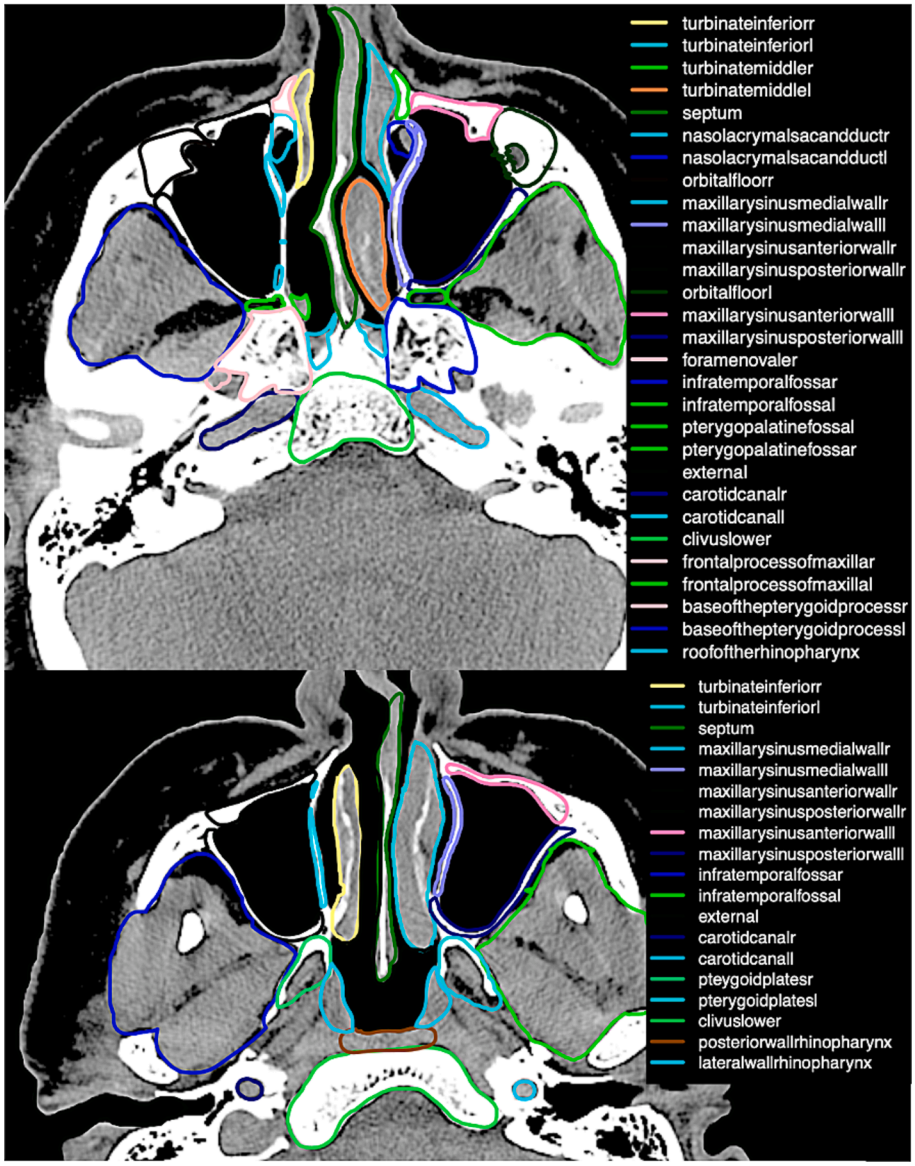

Fig. 3. Caption of the atlas centered on the maxillary sinus.

customize the clinical target volumes and to perform dose-painting in poRT for sinonasal malignancies. This entire process relies on continuous interdisciplinary communication, serving as a vital prerequisite to optimize radiotherapy. The goal is to reduce irradiation volumes while maintaining or even increasing local control, as avoiding local failure becomes imperative when tailoring treatments to minimize radiation-induced morbidity.

Advancements in in-room imaging through surgical navigation systems offer intraoperative support for surgeons, potentially leading to improved rates of safe margins and enhanced oncologic outcomes [35,36]. The precision of the latest generation navigation systems has reached less than 1 mm [37]. Given the intricate proximity of critical structures such as the optic nerves, orbits, optic chiasm, pituitary gland, internal carotid artery, cranial nerves, and the brain to complex anatomical structures, this tool proves instrumental in minimizing surgical morbidity, in a more helpful way if bony structures are involved. Surgical navigation enables the integration of a macroscopic view with precise CT/MRI location, providing a better understanding of the tumor implantation area. Looking ahead, data obtained during intraoperative navigation could be integrated with pre- and postoperative imaging to augment accuracy. Surgeons could use a navigated pointer to delineate the tumor implantation area during surgery, and this delineation could be automatically transferred to postoperative imaging. This integration facilitates the radiation oncologist's understanding of volumes at risk, streamlining the communication of critical information between surgical and radiotherapeutic approaches and allow better dose-painting of the tumor.

The main limitation of this study is that a modified Delphi method is by essence an expert opinion consensus. This study design is required when no data exists in the literature regarding the research question. Despite the scarcity of solid evidence, this study achieved a multidisciplinary consensus aiming to pave the way for a better plan of treatment for sinonasal malignancy by optimizing the poRT dose distribution.

Conclusion

This accurate atlas of structures identified during EESBS could serve for the poRT planning in patients with sinonasal tumors. It might allow, through careful planning of areas at risk of recurrence and adjacent organs to be preserved, to limit the morbidity of poRT while maintaining good local control. This precision-medicine approach would align with the limitation of morbidity allowed by EESBS in comparison with

craniofacial resection. Prospective studies are necessary to rigorously assess the morbidity and outcomes implications of this approach.

Funding

The authors did not receive any external funding.

CRediT authorship contribution statement

Florent Carsuzaa: Writing – review & editing, Writing – original draft, Visualization, Validation, Resources, Methodology, Investigation, Formal analysis, Data curation, Conceptualization. **Valentin Favier:** Writing – review & editing, Writing – original draft, Validation, Formal analysis, Data curation. **Lise Seguin:** Writing – original draft, Resources, Formal analysis, Data curation. **Mario Turri-Zanoni:** Writing – review & editing, Validation, Investigation, Data curation. **Anna-Maria Camarda:** Writing – review & editing, Validation, Formal analysis, Data curation. **Benjamin Verillaud:** Writing – review & editing, Validation, Investigation, Data curation. **Philippe Herman:** Writing – review & editing, Validation, Formal analysis, Data curation. **Daniele Borsetto:** Writing – review & editing, Investigation, Data curation. **Alberto Schreiber:** Writing – review & editing, Investigation, Data curation. **Stefano Taboni:** Writing – review & editing, Investigation, Data curation. **Vittorio Rampinelli:** Writing – original draft, Investigation, Formal analysis. **Alessandro Vinciguerra:** Writing – review & editing, Investigation, Data curation. **Alperen Vural:** Writing – review & editing, Investigation, Data curation. **Xavier Liem:** Writing – review & editing, Investigation, Data curation. **Fabio Busato:** Writing – review & editing, Investigation, Formal analysis. **Sophie Renard:** Writing – review & editing, Investigation, Data curation. **Charles Dupin:** Writing – review & editing, Investigation, Formal analysis. **Mélanie Doré:** Writing – review & editing, Investigation, Data curation. **Pierre Graff:** Writing – review & editing, Investigation, Data curation. **Yungan Tao:** Writing – review & editing, Investigation, Data curation. **Séverine Racadot:** Writing – review & editing, Investigation, Data curation. **Antoine Moya Plana:** Writing – review & editing, Investigation, Formal analysis, Data curation. **Basile N. Landis:** Writing – review & editing, Validation, Formal analysis. **Pierre-Yves Marcy:** Writing – review & editing, Investigation, Data curation. **Vincent Patron:** Writing – review & editing, Investigation, Data curation. **Ludovic de Gabory:** Writing – review & editing, Validation, Formal analysis. **Ester Orlandi:** Writing – original draft, Validation, Supervision, Methodology, Investigation, Data curation. **Marco Ferrari:** Writing – original draft, Validation, Methodology, Investigation, Formal analysis, Data curation. **Juliette Thariat:** Writing – review & editing, Writing – original draft, Validation, Supervision, Software, Resources, Project administration, Methodology, Investigation, Formal analysis, Data curation, Conceptualization.

Declaration of competing interest

The authors declare that they have no known competing financial interests or personal relationships that could have appeared to influence the work reported in this paper.

Appendix A. Supplementary data

Supplementary data to this article can be found online at https://doi.org/10.1016/j.radonc.2025.110784.

References

[1] Baig Mirza A, Ravindran V, Okasha M, et al. Systematic review comparing open versus endoscopic surgery in clival chordomas and a 10-year single-center experience. J Neurol Surg B Skull Base 2022;83(S 02):e113–25. https://doi.org/10.1055/s-0041-1722933.

[2] Raper DMS, Komotar RJ, Starke RM, Anand VK, Schwartz TH. Endoscopic versus open approaches to the skull base: A comprehensive literature review. Oper Tech Otolaryngol Head Neck Surg 2011;22:302–7. https://doi.org/10.1016/j.otot.2011.08.003.

[3] Abergel A. Comparison of quality of life after transnasal endoscopic vs open skull base tumor resection. Arch Otolaryngol Head Neck Surgery 2012;138:142. https://doi.org/10.1001/archoto.2011.1146.

[4] López F, Shah JP, Beitler JJ, et al. The selective role of open and endoscopic approaches for sinonasal malignant tumours. Adv Ther 2022;39:2379–97. https://doi.org/10.1007/s12325-022-02080-x.

[5] Barinsky GL, Azmy MC, Kilic S, et al. Comparison of open and endoscopic approaches in the resection of Esthesioneuroblastoma. Ann Otol Rhinol Laryngol 2021;130:136–41. https://doi.org/10.1177/0003489420939582.

[6] Rutland JW, Gill CM, Ladner T, et al. Surgical outcomes in patients with endoscopic versus transcranial approach for skull base malignancies: a 10-year institutional experience. Br J Neurosurg 2022;36:79–85. https://doi.org/10.1080/02688697.2020.1779659.

[7] Ferrari M, Orlandi E, Bossi P. Sinonasal cancers treatments: state of the art. Curr Opin Oncol 2021;33:196–205. https://doi.org/10.1097/CCO.0000000000000726.

[8] Maggiore G, Fancello1 G, Gasparini A, et al. Temporal evolution of quality of life in patients endoscopically treated for sinonasal malignant tumors. Rhinology 2023;61:231–45. https://doi.org/10.4193/Rhin22.367.

[9] Turri-Zanoni M, Lambertoni A, Margherini S, et al. Multidisciplinary treatment algorithm for the management of sinonasal cancers with orbital invasion: A retrospective study. Head Neck. Published online April 2019:hed.2575doi:10.1002/hed.25759.

[10] Bastier PL, de Gabory L. Design and assessment of an anatomical diagram for sinonasal malignant tumour resection. Rhinology 2016;54:361–7. https://doi.org/10.4193/Rhino15.355.

[11] Fierens S, Moya-Plana A, Vergez S, et al. Do practitioners assess sinonasal adenocarcinoma extension similarly? Interdisciplinary concordance in 21 cases. Clin Otolaryngol 2021;46:665–9. https://doi.org/10.1111/coa.13708.

[12] Carsuzaa F, Favier V, Ferrari M, et al. Need for close interdisciplinary communication after endoscopic endonasal surgery to further personalize postoperative radiotherapy in sinonasal malignancies. Front Oncol 2023;13:1130040. https://doi.org/10.3389/fonc.2023.1130040.

[13] Paré A, Blanchard P, Rosellini S, et al. Outcomes of multimodal management for sinonasal squamous cell carcinoma. J Cranio-Maxill Surg 2017;45:1124–32. https://doi.org/10.1016/j.jcms.2017.05.006.

[14] Hasson F, Keeney S, McKenna H. Research guidelines for the Delphi survey technique. J Adv Nurs 2000;32:1008–15.

[15] French Haute autorité de santé. Elaboration de recommandation de bonne pratique – Recommandations par consensus formalise; 2010.

[16] Fontbonne C, Fontbonne JM, Azemar N. Espadon, an R package for automation, exploitation and processing of DICOM files in medical physics and clinical research. Physica Medica 2023;109:102580. https://doi.org/10.1016/j.ejmp.2023.102580.

[17] Ferrari M, Mattavelli D, Tomasoni M, et al. The MUSES*: a prognostic study on 1360 patients with sinonasal cancer undergoing endoscopic surgery-based treatment: *MUlti-institutional collaborative Study on Endoscopically treated Sinonasal cancers. Eur J Cancer 2022;171:161–82. https://doi.org/10.1016/j.ejca.2022.05.010.

[18] Abiri A, Bitner BF, Nguyen TV, et al. Clinical and technical factors in endoscopic skull base surgery associated with reconstructive success. Rhinology 2024;62:330–41. https://doi.org/10.4193/Rhin23.267.

[19] Leleu T, Bastit V, Doré M, et al. Histosurgical mapping of endoscopic endonasal surgery of sinonasal tumours to improve radiotherapy guidance. Cancer Radiothrapie 2022;26:440–4. https://doi.org/10.1016/j.canrad.2021.06.014.

[20] Grégoire V, Evans M, Le QT, et al. Delineation of the primary tumour Clinical Target Volumes (CTV-P) in laryngeal, hypopharyngeal, oropharyngeal and oral cavity squamous cell carcinoma: AIRO, CACA, DAHANCA, EORTC, GEORCC, GORTEC, HKNPCSG, HNCIG, IAG-KHT, LPRHHT, NCIC CTG, NCRI, NRG Oncology, PHNS, SBRT, SOMERA, SRO, SSHNO, TROG consensus guidelines. Radiother Oncol 2018;126:3–24. https://doi.org/10.1016/j.radonc.2017.10.016.

[21] Brouwer CL, Steenbakkers RJHM, Bourhis J, et al. CT-based delineation of organs at risk in the head and neck region: DAHANCA, EORTC, GORTEC, HKNPCSG, NCIC CTG, NCRI, NRG Oncology and TROG consensus guidelines. Radiother Oncol 2015;117:83–90. https://doi.org/10.1016/j.radonc.2015.07.041.

[22] You R, Liu YP, Chen XZ, et al. Surgical treatment of nasopharyngeal cancer - a consensus recommendation from two Chinese associations. Rhinology 2024;62:23–34. https://doi.org/10.4193/Rhin23.054.

[23] Akazawa K, Doi H, Ohta S, et al. Relationship between Eustachian tube dysfunction and otitis media with effusion in radiotherapy patients. J Laryngol Otol 2018;132(2):111–6. https://doi.org/10.1017/S0022215118000014.

[24] Gera R, Mozzanica F, Karligkiotis A, et al. Lateral lamella of the cribriform plate, a keystone landmark: proposal for a novel classification system. Rhinology 2018;56:65–72. https://doi.org/10.4193/Rhin17.067.

[25] Gotlib T, Kuzminska M, Held-Ziolkowska M, Niemczyk K. Asymmetry of the anterior skull base at the level of frontal ostium, a radioanatomical study. Rhinology 2014;52:419–23. https://doi.org/10.4193/Rhino14.071.

[26] Resteghini C, Castelnuovo P, Nicolai P, et al. The SINTART 1 study. A phase II non-randomised controlled trial of induction chemotherapy, surgery, photon-, proton- and carbon ion-based radiotherapy integration in patients with locally advanced resectable sinonasal tumours. Eur J Cancer 2023;187:185–94. https://doi.org/10.1016/j.ejca.2023.03.033.

[27] Bossi P, Orlandi E, Resteghini C, et al. The SINTART 2 Study. A phase II non-randomised controlled trial of induction chemotherapy, photon-, proton- and carbon-ion-based radiotherapy integration in patients with locally advanced unresectable sinonasal tumours. Eur J Cancer 2023;187:134–43. https://doi.org/10.1016/j.ejca.2023.03.034.

[28] Mauthe T, Holzmann D, Soyka MB, et al. Overall and disease-specific survival of sinonasal adenoid cystic carcinoma: a systematic review and meta-analysis. Rhinology 2023;61:508–18. https://doi.org/10.4193/Rhin23.204.
[29] Homma A, Saheki M, Suzuki F, Fukuda S. Computer image-guided surgery for total maxillectomy. Eur Arch Otorhinolaryngol 2008;265:1521–6. https://doi.org/10.1007/s00405-008-0693-x.
[30] Sunkaraneni VS, Qian H, Wong H, Javer A. Validation of a grading system for the attachment of the superior turbinate to the sphenoid face. Int Forum Allergy Rhinol 2012;2:411–4. https://doi.org/10.1002/alr.21041.
[31] Fukumitsu N, Ishikawa H, Ohnishi K, et al. Dose distribution resulting from changes in aeration of nasal cavity or paranasal sinus cancer in the proton therapy. Radiother Oncol 2014;113:72–6. https://doi.org/10.1016/j.radonc.2014.08.024.
[32] Konuthula N, Perez FA, Maga AM, et al. Automated atlas-based segmentation for skull base surgical planning. Int J Comput Assist 2021;16:933–41. https://doi.org/10.1007/s11548-021-02390-5.
[33] Van Dijk LV, Van Den Bosch L, Aljabar P, et al. Improving automatic delineation for head and neck organs at risk by Deep Learning Contouring. Radiother Oncol 2020;142:115–23. https://doi.org/10.1016/j.radonc.2019.09.022.
[34] Sotiras A, Davatzikos C, Paragios N. Deformable Medical Image Registration: A Survey. IEEE Trans Med Imaging 2013;32:1153–90. https://doi.org/10.1109/TMI.2013.2265603.
[35] Vicaut E, Bertrand B, Betton JL, et al. Use of a navigation system in endonasal surgery: Impact on surgical strategy and surgeon satisfaction. A prospective multicenter study. Eur Ann Otorhinolaryngol Head Neck Dis 2019;136:461–4. https://doi.org/10.1016/j.anorl.2019.08.002.
[36] Taboni S, Ferrari M, Daly MJ, et al. Navigation-guided transnasal endoscopic delineation of the posterior margin for maxillary sinus cancers: a preclinical study. Front Oncol 2021;11:747227. https://doi.org/10.3389/fonc.2021.747227.
[37] Grauvogel TD, Engelskirchen P, Semper-Hogg W, Grauvogel J, Laszig R. Navigation accuracy after automatic- and hybrid-surface registration in sinus and skull base surgery. PLoS One1 2017;12. https://doi.org/10.1371/journal.pone.0180975. e0180975.